Mapping the hydrodynamic response to the initial geometry in heavy-ion collisions

Fernando G. Gardim,[1] Frédérique Grassi,[1] Matthew Luzum,[2] and Jean-Yves Ollitrault[2]
[1]*Instituto de Física, Universidade de São Paulo, C.P. 66318, 05315-970, São Paulo-SP, Brazil*
[2]*CNRS, URA2306, IPhT, Institut de physique théorique de Saclay, F-91191 Gif-sur-Yvette, France*
(Received 29 November 2011; published 24 February 2012)

We investigate how the initial geometry of a heavy-ion collision is transformed into final flow observables by solving event-by-event ideal hydrodynamics with realistic fluctuating initial conditions. We study quantitatively to what extent anisotropic flow (v_n) is determined by the initial eccentricity ε_n for a set of realistic simulations, and we discuss which definition of ε_n gives the best estimator of v_n. We find that the common practice of using an r^2 weight in the definition of ε_n in general results in a poorer predictor of v_n than when using r^n weight, for $n > 2$. We similarly study the importance of additional properties of the initial state. For example, we show that in order to correctly predict v_4 and v_5 for noncentral collisions, one must take into account nonlinear terms proportional to ε_2^2 and $\varepsilon_2\varepsilon_3$, respectively. We find that it makes no difference whether one calculates the eccentricities over a range of rapidity or in a single slice at $z = 0$, nor is it important whether one uses an energy or entropy density weight. This knowledge will be important for making a more direct link between experimental observables and hydrodynamic initial conditions, the latter being poorly constrained at present.

DOI: 10.1103/PhysRevC.85.024908 PACS number(s): 25.75.Ld, 24.10.Nz

I. INTRODUCTION

Anisotropic flow [1] is one of the most important probes of ultrarelativistic nucleus-nucleus collisions. While early studies [2] focused on elliptic flow generated by the almond shape of the interaction region in noncentral collisions, most of the recent activity concerns the effect of fluctuations in the initial geometry [3]. Such fluctuations result in fluctuations of elliptic flow [4] and in new types of flow, such as triangular flow [5] and higher harmonics. These new flow observables have been recently measured at the Relativistic Heavy Ion Collider (RHIC) [6,7] and the Large Hadron Collider [8–11].

Flow phenomena are best modeled with ideal [12] or viscous [13] hydrodynamics. Event-by-event hydrodynamics [14] provides a natural way of studying flow fluctuations: One typically supplies a set of initial conditions, evolves these initial conditions through ideal [14–18] or viscous [19] hydrodynamics, and then computes particle emission at the end. Observables are finally averaged over a large number of initial conditions, much in the same way as they are averaged over events in an actual experiment.

The largest source of uncertainty in these hydrodynamic models is the initial conditions [20,21], that is, the state of the system after which it has sufficiently thermalized or isotropized for the hydrodynamic description to be valid. Several models of initial geometry fluctuations have been proposed [22–26]. The usual procedure is to choose one or two of these simple models for the initial conditions and calculate the resulting flow observables. Significant progress has been made recently by simultaneously comparing to several of the newly measured flow observables. With this approach, hydrodynamic calculations can be used to rule out a particular model of initial conditions if results do not match experimental data [6,27,28]. But it does not tell us *why* a particular model fails. In order to constrain the initial state directly from data, we need to identify which properties of the initial state determine a given observable. These constraints can then provide valuable guidance in the construction of better, more sophisticated models of the early-time dynamics.

It is well known that elliptic flow is largely determined by the participant eccentricity [4]. Teaney and Yan [29] have introduced a cumulant expansion of the initial density profile, in which the participant eccentricity is only the first term in an infinite series, and they have suggested that the hydrodynamic response may be improved by adding higher-order terms, but to our knowledge their suggestion has never been checked quantitatively. Other expansions have also been suggested [30]. As for triangular flow, v_3, symmetry considerations have been used to argue that it should be created by an initial triangularity ε_3, but several definitions of ε_3 are in use [5,31] and it has never been investigated which is a better predictor of v_3. Finally, it has been shown that higher harmonics [18,32] v_4 and v_5 are in general *not* proportional to the corresponding ε_4 and ε_5. A possible better estimator was recently suggested [33], but it has not been checked quantitatively.

The goal of this paper is to improve our understanding of the hydrodynamic response to initial fluctuations. We carry out event-by-event ideal hydrodynamic calculations with realistic initial conditions and then quantitatively compare the final values of v_n with estimates derived from the initial density profile. We are, thus, able to systematically determine the best estimators of flow observables v_n, $n = 2$–5 from the initial transverse density profile.

II. A SYSTEMATIC APPROACH TO CHARACTERIZING THE HYDRODYNAMIC RESPONSE

In hydrodynamics, the momentum distribution of particles at the end of the evolution is completely determined by initial conditions. Current models of initial conditions predict the system at early times to consist of flux tubes or other stringlike structures that are extended longitudinally [34], with an approximate boost invariance at midrapidity. Most models

also predict that the initial transverse flow, if any, is small [35,36] (except for possible fluctuations of the initial flow velocity [37]). Under these approximations, any observable is a completely deterministic functional of the transverse energy density profile $\rho(x, y)$.

This density in turn can be completely characterized by a set of complex moments [29]

$$\begin{aligned} W_{p+q,p-q} &\equiv \int (x+iy)^p (x-iy)^q \rho(x,y)dxdy \\ &= \int r^{p+q} e^{i(p-q)\phi} \rho(r\cos\phi, r\sin\phi) r dr d\phi \\ &\equiv W_{0,0}\{r^{p+q} e^{i(p-q)\phi}\}, \end{aligned} \tag{1}$$

where $\{\cdots\}$ denotes an average value over the transverse plane weighted by $\rho(x, y)$. Small values of the first index $(p + q)$ correspond to small powers of $|\vec{k}|$ in a two-dimensional Fourier transform of $\rho(x, y)$, and, thus, describe large-scale structure, while moments with larger values are more sensitive to small-scale structure. The second index indicates the rotational symmetry of each moment.

If the system has $\phi \to \phi + \pi$ symmetry, all odd moments (i.e., with $p - q$ odd) vanish. In a symmetric heavy-ion collision, the symmetry between target and projectile implies an approximate $\phi \to \phi + \pi$ symmetry in a centered coordinate system defined by $W_{1,1} = 0$ (used throughout this article). This symmetry is broken only by quantum fluctuations in the wave function of incoming nuclei [5]. Therefore, odd moments are typically small relative to even moments. Similarly, central heavy-ion collisions are rotationally symmetric except for fluctuations, so all moments with $p \neq q$ are small. For semicentral or peripheral collisions, however, the interaction area is almond shaped [2], resulting in sizable moments in the second Fourier harmonic $p - q = 2$. For example, the familiar participant eccentricity ε_2 and participant plane Φ_2 are defined by Ref. [4]

$$\varepsilon_2 e^{2i\Phi_2} \equiv -\frac{W_{2,2}}{W_{2,0}} = -\frac{\{r^2 e^{2i\phi}\}}{\{r^2\}}. \tag{2}$$

The value of ε_2 is typically 0.3 in a semicentral heavy-ion collision: anisotropies are small, and so it is natural to expect that the hydrodynamic response can be ordered into a Taylor's series. Higher-order even harmonics are smaller: The fourth-order anisotropy $\varepsilon_4 \equiv |W_{4,4}|/W_{4,0}$ is typically of order $(\varepsilon_2)^2$ [38], so it can be treated in practice as a higher-order term in a Taylor series expansion.

Any observable can generally be written as a function of moments of ρ. In this paper, we focus on anisotropic flow, v_n, which, along with the event-plane angle Ψ_n, is defined by

$$v_n e^{in\Psi_n} = \{e^{in\phi_p}\}. \tag{3}$$

Here $\{\cdots\}$ denotes an average over the distribution of particle momenta in one event. In hydrodynamics, this is a smooth (boosted thermal) probability distribution. In a real-world collision, v_n and Ψ_n must be inferred from a finite sample of particles. The resulting statistical error makes an event-by-event determination of v_n impossible in current experiments—only event-averaged quantities are reliable. In theoretical calculations, however, we can accurately determine v_n and Ψ_n in every event in order to study precisely how they depend on initial conditions.

The symmetries of v_n restrict what combinations of moments of the initial distribution it can depend on. For example, to first order in anisotropies, the rotational symmetry of v_n implies that it is a linear combination of moments in the same harmonic:

$$v_n e^{in\Psi_n} = \sum_{p=0}^{\infty} k_{n+2p,n} W_{n+2p,n}, \tag{4}$$

where the coefficients $k_{n+2p,n}$ are (dimensionful) functions of (the infinite set of) rotationally symmetric moments $W_{2m,0}$. The conventional eccentricity scaling of elliptic flow, $n = 2$, amounts to truncating the series to the first term, $p = 0$, i.e., the statement that $v_2 \propto \varepsilon_2$ is a statement that the hydrodynamic response is sensitive only to the large-scale structure of the initial density distribution, with the response to small-scale structure damped in comparison. This statement has not been quantitatively tested until now. Teaney and Yan [29] have suggested that including a higher-order term $p = 1$ in addition to the lowest order may improve the accuracy (actually, they listed cumulants instead of moments, but it is equivalent). This hypothesis will be checked quantitatively in Sec. IV.

In this work we will use the following notation for the dimensionless eccentricity $\varepsilon_{m,n}$ and the corresponding orientation angle $\Phi_{m,n}$ in a given event:

$$\varepsilon_{m,n} e^{in\Phi_{m,n}} \equiv -\frac{\{r^m e^{in\phi}\}}{\{r^m\}}, \tag{5}$$

and we use the shorthand notations $\varepsilon_n \equiv \varepsilon_{n,n}$, $\Phi_n \equiv \Phi_{n,n}$. If $m - n$ is even and positive, the numerator of Eq. (5) is $W_{m,n}/W_{0,0}$. If m is even, the denominator is $W_{m,0}/W_{0,0}$.

Gubser and Yarom have proposed a different basis for the expansion [30], which can be seen as a partial resummation of the infinite series (4). To first order in anisotropies, they write $v_n e^{in\Psi_n} \propto f_n e^{in\Phi_n^{\mathrm{GY}}}$, where f_n and Φ_n^{GY} are solely determined by the initial density profile. The first harmonics are given by

$$\begin{aligned} f_1 e^{i\Phi_1^{\mathrm{GY}}} &= -\left\{\frac{q r e^{i\phi}}{1+q^2r^2}\right\} \\ f_2 e^{2i\Phi_2^{\mathrm{GY}}} &= -\left\{\frac{q^2 r^2 e^{2i\phi}}{1+q^2r^2}\right\} \\ f_3 e^{3i\Phi_3^{\mathrm{GY}}} &= -\left\{\frac{q^3 r^3 e^{3i\phi}}{(1+q^2r^2)^2}\right\}, \end{aligned} \tag{6}$$

with $q^2 \equiv 1/\{r^2\} = W_{0,0}/W_{2,0}$. Strictly speaking, this expansion scheme is of obvious relevance only for a conformal equation of state and for a particular initial density profile falling more slowly at large r than realistic profiles. Nevertheless, we find it instructive to test how this expansion compares with conventional eccentricity scaling with realistic initial conditions. Finally, one can also consider moments of the entropy density profile instead of energy density, which we also test in the following.

The goal here is to determine which moment or combination of moments serve as a best estimator for flow observables v_n with $n = 2$–5. We shall see, in particular, that v_4 and v_5 are not well described by the leading-order expansion [Eq. (4)]

and require nonlinear terms, which are also constrained by symmetry. Note that symmetry considerations alone exclude a linear mixing between the second and third harmonics, as proposed in Ref. [39].

III. DETERMINING THE BEST ESTIMATOR OF v_n

The goal of this work is to test to what extent v_n and Ψ_n are correlated with quantities derived from the initial transverse density distribution, such as ε_n and Φ_n. Previously, the correlation of anisotropic flow with the initial geometry has been studied by plotting the distribution of $\Psi_n - \Phi_n$ [16,18,31] or by displaying a scatter plot of v_n versus ε_n [40]. In this paper, we carry out a global analysis which studies both aspects simultaneously and quantitatively.

For a given event, we write

$$v_n e^{in\Psi_n} = k\varepsilon_n e^{in\Phi_n} + \mathcal{E}, \tag{7}$$

where k is an unknown proportionality constant. The first term in the right-hand side defines the estimate for v_n from the initial eccentricity, and the last term $\mathcal{E}$ is the difference between the calculated flow and the proposed estimator or the error in the estimate (note that $\mathcal{E}$ is complex). No known estimator can perfectly predict v_n in every event (for example, two events with the same triangularity can be constructed to have very different triangular flow [32,41]). The best estimator, then, should be defined as the one that minimizes the mean square error $\langle|\mathcal{E}|^2\rangle$, where $\langle\cdots\rangle$ denotes an average over events in a centrality class. A straightforward calculation shows that the best value of k is

$$k = \frac{\langle \varepsilon_n v_n \cos[n(\Psi_n - \Phi_n)]\rangle}{\langle \varepsilon_n^2\rangle}. \tag{8}$$

Inserting Eq. (8) into Eq. (7), one obtains the best estimator of v_n from ε_n in a centrality class. Using Eqs. (7) and (8), one finally derives the mean-square error

$$\langle|\mathcal{E}|^2\rangle = \langle v_n^2\rangle - k^2\langle\varepsilon_n^2\rangle. \tag{9}$$

This shows that the rms value of the best estimator, $|k|\sqrt{\langle\varepsilon_n^2\rangle}$, is always smaller than the rms value of v_n. In the next section, we compute $k\sqrt{\langle\varepsilon_n^2\rangle}/\sqrt{\langle v_n^2\rangle}$ for various definitions of ε_n and several values of n. The closer the ratio to 1, the better the estimate. Using Eq. (9), a ratio of 0.95 corresponds to a rms error of 31%. A change of sign in the ratio signals that the estimator is anticorrelated to v_n.

According to the discussion in Sec. II, an improved estimator may be obtained by adding more terms in Eq. (7), e.g.,

$$v_n e^{in\Psi_n} = k\varepsilon_n e^{in\Phi_n} + k'\varepsilon_n' e^{in\Phi_n'} + \mathcal{E}, \tag{10}$$

where ε_n' and Φ_n' are other quantities determined from the initial density profile (for example, the next higher cumulant). The best estimator is now given by the following system of equations:

$$\begin{aligned}\langle \varepsilon_n v_n \cos[n(\Psi_n - \Phi_n)]\rangle &= k'\langle \varepsilon_n\varepsilon_n' \cos[n(\Phi_n' - \Phi_n)]\rangle + k\langle\varepsilon_n^2\rangle\\ \langle \varepsilon_n' v_n \cos[n(\Psi_n - \Phi_n')]\rangle &= k\langle \varepsilon_n\varepsilon_n' \cos[n(\Phi_n - \Phi_n')]\rangle + k'\langle\varepsilon_n'^2\rangle,\end{aligned} \tag{11}$$

which can be solved for k and k'. The rms value of the best estimator and the rms error are related by an equation analogous to Eq. (9):

$$\langle|\mathcal{E}|^2\rangle = \langle v_n^2\rangle - \langle|k\varepsilon_n e^{in\Phi_n} + k'\varepsilon_n' e^{in\Phi_n'}|^2\rangle. \tag{12}$$

One can show that the rms error is always smaller with two terms, Eq. (12), than with only one of the terms, Eq. (9). This is intuitive if one thinks of Eqs. (7) and (10) as fits to v_n: adding more parameters improves the quality of the fit.

IV. RESULTS

We simulate Au-Au collisions at the top RHIC energy using the hydrodynamic code NeXSPheRIO [14]. NeXSPheRIO solves the equations of relativistic ideal hydrodynamics using initial conditions provided by the event generator NeXus [42]. Fluctuations in initial conditions are studied by generating 150 NeXus events in each of the 10% centrality classes studied and solving the equations of ideal hydrodynamics independently for each event. In addition, 115 NeXus events with zero impact parameter were used in order to study very central collisions. NeXSPheRIO provides a good description of rapidity and transverse momentum spectra [43] and elliptic flow v_2 [44]. In addition, it reproduces the long-range structures observed in two-particle correlations [45].

The code NeXSPheRIO emits particles at the end of the hydrodynamical evolution using a Monte Carlo generator. Anisotropic flow v_n, and the corresponding event-plane angle Ψ_n are defined from Eq. (3), where $\{\cdots\}$ denotes an average over all particles in the pseudorapidity interval $-1 < \eta < 1$.

This work requires an accurate determination of v_n in each hydrodynamic event, and so associated with each initial condition, we generate approximately 6×10^5 particles by computing particle production with N Monte Carlos. This allows for a much better event plane resolution and much smaller statistical error (the actual multiplicity in an event is $\approx 6 \times 10^5/N$). We compute v_2 to v_5. We do not compute v_1 because it changes sign as a function of transverse momentum [40], so an average with equal weighting such as in Eq. (3) is not appropriate [46]. An analysis of directed flow is left to future work. The relative statistical errors on v_2 to v_5 in a given event are 3.7%, 5.7%, 9.8%, and 20%, respectively. The rms error on the event planes Ψ_2 to Ψ_5 are 1°, 1°, 1.5°, and 2°. This means that the event-plane resolution [47] for v_5 is as large as 0.98 and even closer to 1 for all other harmonics.

In such a three-dimensional calculation, there is more than one way to define the transverse energy density profile that is used as a weight when calculating the eccentricities in Eq. (5). We show results obtained by averaging over the transverse energy density profile at $z = 0$ (i.e., central space-time rapidity $\eta_s = 0$). Though the results are not shown, we have found that averaging over the space-time rapidity interval $-1 < \eta_s < 1$ results in predictors of equal quality.

It should be noted that the error from these predictors is likely to be larger in our calculations than in many others, for several reasons. First, our hydrodynamical calculations are based on NeXus initial conditions which contain (fluctuating) initial flow, as well as longitudinal fluctuations, and so the

final flow measured in a particular pseudorapidity window is not entirely determined by the initial transverse geometry. In addition, there are statistical fluctuations from the finite number of particles generated at the end of the hydro evolution. These issues set a limit on the rms error introduced in Sec. III, which cannot go to zero. A hydrodynamic calculation with less or no initial flow, in 2+1 dimensions, or that calculates flow from a continuous distribution at freeze-out, though perhaps less realistic, will likely result in a smaller error for the same estimator. Likewise, a nonzero viscosity may cause higher-order cumulants to decrease in importance, improving the predictive power of the lowest moments ε_n. In this sense, these results represent something of a worst-case scenario.

A. Elliptic flow

Elliptic flow is usually thought of as a hydrodynamic response to the initial eccentricity: $v_2 e^{2i\Psi_2} = k\varepsilon_2 e^{2i\Phi_2}$, where the resulting event plane Ψ_2 approximately coincides with the participant plane Φ_2 [4]. The right-hand side of this equation defines an estimator of v_2.

Figure 1 displays the ratio of the rms value of the best estimator to the rms value of the calculated v_2 as a function of centrality. The proportionality constant k is determined using Eq. (8) independently for each centrality class. For central collisions, where all anisotropies are due to fluctuations, the best estimator is able to reproduce over 80% of v_2. This means that the participant eccentricity correctly captures the physics of v_2 fluctuations but that the event-plane Ψ_2 fluctuates around the participant plane Φ_2 [16,18,31] and/or that v_2 has sizable fluctuations for a given ε_2. For midcentral collisions, elliptic flow is driven by the almond-shaped overlap area; therefore, fluctuations are smaller and the estimate is better. The value of k slightly decreases with centrality but very slowly. It is approximately equal to 0.16. Note that k does not represent the ratio of the magnitudes v_2/ε_2 in a typical collision and

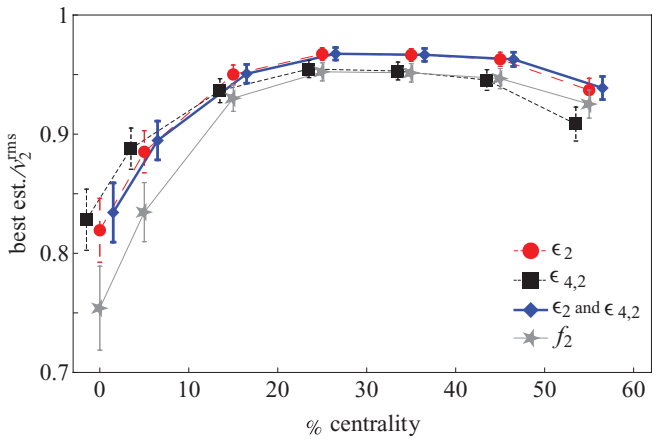

FIG. 1. (Color online) Best estimator for elliptic flow divided by rms v_2 for various combinations of moments of the initial energy density. The leftmost points correspond to 115 events with exactly zero impact parameter. Error bars represent statistical uncertainty from the finite number of events. Diamonds (squares) have been given an x offset of 1.5 (-1.5) for readability.

should be compared neither with v_2/ε_2 obtained from smooth initial conditions nor to the ratio of the average elliptic flow to the average eccentricity v_2/ε_2 which are both larger [27].

As explained in Sec. II, the participant eccentricity is one term out of an infinite series of moments (or cumulants) allowed by symmetry. There is no fundamental reason why the first term in Eq. (4) must be more important than higher-order terms. In order to check quantitatively this issue, we define another estimator of v_2, corresponding to the term $p = 1$ in Eq. (4): $v_2 e^{2i\Psi_2} = k\varepsilon_{4,2} e^{2i\Phi_{4,2}}$. The difference with usual participant eccentricity scaling is that larger values of r are given more weight. As shown in Fig. 1, this estimate is essentially as good as the usual participant eccentricity. A closer look reveals that it is slightly better for central collisions, and slightly worse for noncentral collisions. This means that v_2 is driven more by the periphery of the fireball for central collisions than for peripheral collisions. The result that, for central collisions, anisotropic flow v_n is sensitive to the geometry of the outer layers of the system is in agreement with Refs. [32,48]. There is a limit, however. We have checked that $\varepsilon_{6,2}$ gives a worse estimate than $\varepsilon_{4,2}$ for all centralities, indicating that higher-order moments, and, thus, the extreme periphery, are indeed less important.

Using entropy density instead of energy density to calculate moments also gives a somewhat greater weight to larger r. Indeed, we have found that, calculating ε_2 with an entropy density weight gives results (not shown) that are between the results for ε_2 and $\varepsilon_{4,2}$; that is, slightly better for central collisions and slightly worse for peripheral collisions, but, in general, the result is very close to the result for ε_2 calculated using energy density. In general, either predictor appears to be essentially as good as the other.

Next, we test if the quality of the estimator is improved by combining ε_2 and $\varepsilon_{4,2}$, as in Eq. (10). The improvement is marginal, which means that adding the next term in the cumulant expansion [29] does not significantly improve the determination of the event plane from initial conditions. This implies that the small-scale structure of the initial conditions is unlikely to be responsible for the part of elliptic flow that is not explained by ε_2 and that most of the deviation from being a perfect predictor is likely coming from another source, e.g., nonlinear terms or fluctuating initial flow.

Finally, we test Gubser's estimator, the second line of Eq. (6). This particular quantity gives less weight to the periphery. This makes the estimator much worse for central collisions, as expected from the discussion above, but it is also worse at all other centralities. Overall, ε_2 calculated with energy or entropy density weighting is a very good predictor of v_2, while other quantities that are significantly more sensitive to the periphery compared to the center of the system, or vice versa, are worse.

B. Triangular flow

Similar to elliptic flow and eccentricity, triangular flow v_3 is thought to be a hydrodynamic response to an initial "triangularity" in the initial state: to define the triangularity, Alver and Roland [5] originally suggested $\varepsilon_{2,3}$ [following the

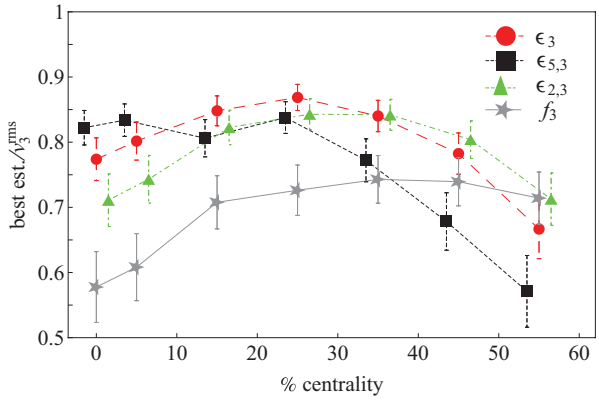

FIG. 2. (Color online) Best estimator for triangular flow divided by rms v_3 for various definitions of ε_3. The leftmost points correspond to 115 events with exactly zero impact parameter. Error bars represent statistical uncertainty from the finite number of events. Triangles (squares) have been given an x offset of 1.5 (-1.5) for readability.

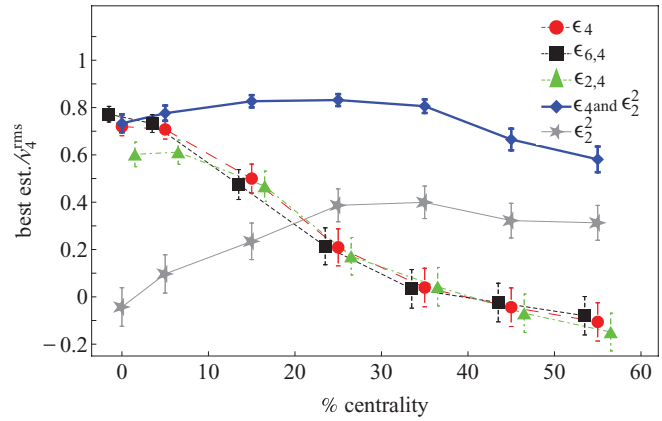

FIG. 3. (Color online) Best estimator for quadrangular flow divided by rms v_4 for various choices of the estimator. Negative values indicate an anticorrelation with the estimator. The leftmost points correspond to 115 events with exactly zero impact parameter. Error bars represent statistical uncertainty from the finite number of events. Triangles (squares) have been given an x offset of 1.5 (-1.5) for readability.

notation of Eq. (5)]. However, the numerator cannot be simply expressed in terms of the moments [Eq. (1)]. Recently it has been more common to use $\varepsilon_{3,3}$ [31], which we denote by ε_3. In this case, the numerator is $W_{3,3}/W_{0,0}$, but the denominator $\{r^3\}$ is not a simple moment. One could instead replace $\{r^3\}$ with a power of the lowest moment $\{r^2\}^{3/2}$. This gives an almost indistinguishable result in our analysis, so we only show the curve for the "standard" denominator.[1]

Figure 2 shows the ratio of the rms value of the best estimator to the rms value of the calculated v_3. The triangularity $\varepsilon_{2,3}$ is a worse predictor of v_3 than ε_3 below 30% centrality but slightly better above 40%. As with v_2, the second-lowest moment $\varepsilon_{5,3}$ is a slightly better predictor for central collisions but worse for noncentral collisions, while $\varepsilon_{7,3}$ (not shown) is worse everywhere. This, again, signals a somewhat stronger sensitivity to the periphery of the collision region in central collisions than in peripheral collisions, though, again, the moment f_3, which has a strong sensitivity to the interior, is worse at all centralities. As with elliptic flow, replacing an energy density weight with an entropy density weight in the calculation of ε_3 gives results (not shown) that are slightly better for central collisions and worse for peripheral collisions but that are essentially equivalent. Finally, using a sum of the lowest two moments ε_3 and $\varepsilon_{5,3}$ (not shown) reproduces the highest points on the figure, i.e., it shows no improvement over the term that is individually the best predictor, except above 40% centrality, where it follows the $\varepsilon_{2,3}$ result. Thus, ε_3 is a very good predictor, with slightly too little sensitivity to the periphery in central collisions and slightly too much in peripheral collisions, but quantities with too-different r dependence are worse.

[1]Values of ε_3 are slightly larger with $\{r^2\}^{3/2}$ than with $\{r^3\}$ denominator, and ε_3 is no longer bounded by 1, but this is almost exactly compensated by the smaller value of k from Eq. (8).

C. Quadrangular flow

Like the triangularity, the quadrangularity has inconsistent definition in the literature. Some authors use $\varepsilon_{2,4}$ [27], and others use $\varepsilon_{4,4}$ (which we denote by ε_4) [38]. Another possible choice is, in the latter case, to replace $\{r^4\}$ with $\{r^2\}^2$ in the denominator. In this case, the estimator is equally good, and so the results are not shown with the rest of the results in Fig. 3.

These results differ qualitatively from our results for v_2 and v_3. For v_2 and v_3, all the estimators we have tested give good results, for all centralities. By contrast, ε_4 gives reasonable predictions only for central collisions. The agreement becomes much worse for peripheral collisions, in agreement with previous analysis [18]. In fact, v_4 is anticorrelated with ε_4 for the most peripheral points. Despite suggested scaling similarities between the centrality dependence of ε_4 and v_4 [38]; this shows that ε_4 cannot be used as an estimator of v_4 on an event-by-event basis for noncentral collisions.

When using an r^2 weight ($\varepsilon_{2,4}$), the result is significantly worse for central collisions. Using the next highest moment $\varepsilon_{6,4}$ is slightly better for central collisions, but all higher moments are worse.

For peripheral collisions, the asymmetry of the nuclear overlap region causes ε_2 to be significantly larger than other moments such as ε_4. This raises the possibility that nonlinear terms involving ε_2 may be important. The first such term allowed by symmetry is proportional to ε_2^2—that is, $k(\varepsilon_2 e^{2i\Phi_2})^2$ [33]. Figure 3 shows that, indeed, this term alone provides a reasonable estimator for noncentral collisions. More interestingly, including both terms, i.e.,

$$v_4 e^{4i\Psi_4} = k\varepsilon_4 e^{4i\Phi_4} + k'\varepsilon_2^2 e^{4i\Phi_2}, \tag{13}$$

results in an excellent predictor for all centralities. For central collisions, ε_4 and ε_2 are both small and of the same order of magnitude, so the first term dominates. For all other centralities, both terms are of comparable magnitudes, and the

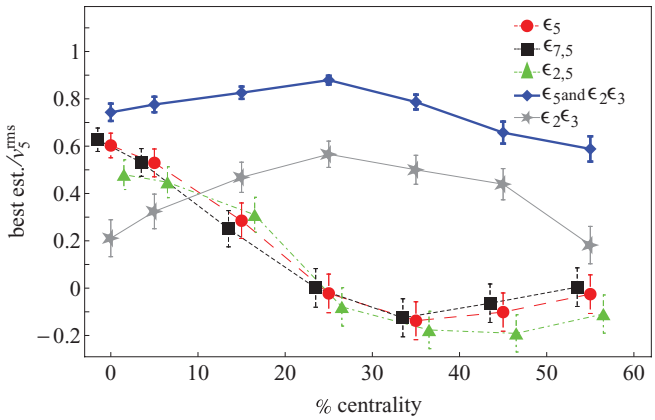

FIG. 4. (Color online) Best estimator for pentagonal flow divided by rms v_5 for various choices of the estimator. Negative values indicate an anticorrelation with the estimator. The leftmost points correspond to 115 events with exactly zero impact parameter. Error bars represent statistical uncertainty from the finite number of events. Triangles (squares) have been given an x offset of 1.5 (-1.5) for readability.

combination gives a much better result than either individual term.

Note that the rms v_4 was measured in 2011 [6,9–11]. In earlier analyses, v_4 was determined with respect to the event plane from elliptic flow [49,50]. The measured quantity is then $\langle v_4 e^{4i\Psi_4} v_2^2 e^{-4i\Psi_2}\rangle/\langle v_2^2\rangle$ [51], not the rms v_4.

D. Pentagonal flow

Figure 4 shows the results for v_5, which are very similar to the results for v_4. Here, the nonlinear term $\varepsilon_2\varepsilon_3$ becomes important even for central collisions. The predictor

$$v_5 e^{5i\Psi_5} = k\varepsilon_5 e^{5i\Phi_5} + k'\varepsilon_2 e^{2i\Phi_2}\varepsilon_3 e^{3i\Phi_3}, \qquad (14)$$

does an excellent job at all centralities.

V. CONCLUSIONS

In this work, we have quantitatively tested to what extent anisotropic flow can be predicted from the initial density profile in event-by-event ideal hydrodynamics with realistic initial conditions. We have shown that the participant eccentricity ε_2 gives a very good prediction of elliptic flow for all centralities. We have also shown that the definition of ε_3 with r^3 weights [29,31] gives a better prediction of triangular flow than the previous definition with r^2 weights. Gubser's moments [30] give worse results for both v_2 and v_3. Higher harmonics v_4 and v_5 can be well predicted from the corresponding eccentricities ε_4 and ε_5 (again defined with r^4 and r^5 weights rather than with r^2 weights) only for central collisions. For noncentral collisions, a good predictor of v_4 must include two terms, proportional to ε_4 and ε_2^2. Likewise, v_5 has contributions proportional to ε_5 and $\varepsilon_2\varepsilon_3$. Defining the eccentricities with energy or entropy density, or using the density at a midrapidity slice or over a finite longitudinal range, is largely a matter of preference and does not make a significant difference.

These results provide an improved understanding of the hydrodynamic response to the initial state in realistic heavy-ion collisions and provide a more direct link between experimental data and properties of the initial stage of the collision. This will allow for the construction of more realistic models for the early-time collision dynamics and, thus, a significant reduction in the systematic uncertainties of extracted bulk properties of the system.

ACKNOWLEDGMENTS

This work is funded by "Agence Nationale de la Recherche" under Grant No. ANR-08-BLAN-0093-01, by Cofecub under project Uc Ph 113/08;2007.1.875.43.9, by FAPESP under projects 09/50180-0 and 09/16860-3, and by CNPq under project 301141/2010-0. M.L. is supported by the European Research Council under the Advanced Investigator Grant No. ERC-AD-267258.

[1] S. A. Voloshin, A. M. Poskanzer, and R. Snellings, arXiv:0809.2949 [nucl-ex].
[2] J.-Y. Ollitrault, Phys. Rev. D **46**, 229 (1992).
[3] M. Miller and R. Snellings, arXiv:nucl-ex/0312008.
[4] B. Alver *et al.* (PHOBOS Collaboration), Phys. Rev. Lett. **98**, 242302 (2007).
[5] B. Alver and G. Roland, Phys. Rev. C **81**, 054905 (2010); **82**, 039903(E) (2010).
[6] A. Adare *et al.* (PHENIX Collaboration), Phys. Rev. Lett. **107**, 252301 (2011).
[7] P. Sorensen (STAR Collaboration), J. Phys. G **38**, 124029 (2011).
[8] K. Aamodt *et al.* (ALICE Collaboration), Phys. Rev. Lett. **107**, 032301 (2011).
[9] K. Aamodt *et al.* (ALICE Collaboration), Phys. Lett. B **708**, 249 (2012).
[10] J. Jia, J. Phys. G **38**, 124012 (2011).
[11] W. Li (CMS Collaboration), J. Phys. G **38**, 124027 (2011).
[12] P. Huovinen and P. V. Ruuskanen, Annu. Rev. Nucl. Part. Sci. **56**, 163 (2006).
[13] P. Romatschke, Int. J. Mod. Phys. E **19**, 1 (2010).
[14] Y. Hama, T. Kodama, and O. J. Socolowski, Braz. J. Phys. **35**, 24 (2005).
[15] H. Petersen, J. Steinheimer, G. Burau, M. Bleicher, and H. Stocker, Phys. Rev. C **78**, 044901 (2008).
[16] H. Holopainen, H. Niemi, and K. J. Eskola, Phys. Rev. C **83**, 034901 (2011).
[17] K. Werner, I. Karpenko, T. Pierog, M. Bleicher, and K. Mikhailov, Phys. Rev. C **82**, 044904 (2010).
[18] Z. Qiu and U. W. Heinz, Phys. Rev. C **84**, 024911 (2011).
[19] B. Schenke, S. Jeon, and C. Gale, Phys. Rev. Lett. **106**, 042301 (2011).
[20] M. Luzum and P. Romatschke, Phys. Rev. C **78**, 034915 (2008); **79**, 039903(E) (2009).
[21] U. W. Heinz, C. Shen, and H. Song, arXiv:1108.5323 [nucl-th].
[22] W. Broniowski, M. Rybczynski, and P. Bozek, Comput. Phys. Commun. **180**, 69 (2009).
[23] H.-J. Drescher and Y. Nara, Phys. Rev. C **76**, 041903 (2007).

[24] B. Alver, M. Baker, C. Loizides, and P. Steinberg, arXiv:0805.4411 [nucl-ex].
[25] C. Flensburg, arXiv:1108.4862 [nucl-th].
[26] B. Muller and A. Schafer, arXiv:1111.3347 [hep-ph].
[27] B. H. Alver, C. Gombeaud, M. Luzum, and J.-Y. Ollitrault, Phys. Rev. C **82**, 034913 (2010).
[28] Z. Qiu, C. Shen, and U. W. Heinz, Phys. Lett. B **707**, 151 (2012).
[29] D. Teaney and L. Yan, Phys. Rev. C **83**, 064904 (2011).
[30] S. S. Gubser and A. Yarom, Nucl. Phys. B **846**, 469 (2011).
[31] H. Petersen, G. Y. Qin, S. A. Bass, and B. Muller, Phys. Rev. C **82**, 041901 (2010).
[32] F. G. Gardim, Y. Hama, and F. Grassi, arXiv:1110.5658 [nucl-th].
[33] M. Luzum, J. Phys. G **38**, 124026 (2011).
[34] A. Dumitru, F. Gelis, L. McLerran, and R. Venugopalan, Nucl. Phys. A **810**, 91 (2008).
[35] W. Broniowski, M. Chojnacki, W. Florkowski, and A. Kisiel, Phys. Rev. Lett. **101**, 022301 (2008).
[36] J. Vredevoogd and S. Pratt, Phys. Rev. C **79**, 044915 (2009).
[37] S. Florchinger and U. A. Wiedemann, J. High Energy Phys.11 (2011) 100.
[38] R. A. Lacey, R. Wei, J. Jia, N. N. Ajitanand, J. M. Alexander, and A. Taranenko, Phys. Rev. C **83**, 044902 (2011).
[39] G. Y. Qin, H. Petersen, S. A. Bass, and B. Muller, Phys. Rev. C **82**, 064903 (2010).
[40] F. G. Gardim, F. Grassi, Y. Hama, M. Luzum, and J.-Y. Ollitrault, Phys. Rev. C **83**, 064901 (2011).
[41] R. P. G. Andrade, F. Gardim, F. Grassi, Y. Hama, and W. L. Qian, J. Phys. G **38**, 124123 (2011).
[42] H. J. Drescher, M. Hladik, S. Ostapchenko, T. Pierog, and K. Werner, Phys. Rep. **350**, 93 (2001).
[43] W. L. Qian, R. Andrade, F. Grassi, O. J. Socolowski, T. Kodama, and Y. Hama, Int. J. Mod. Phys. E **16**, 1877 (2007).
[44] R. P. G. Andrade, F. Grassi, Y. Hama, T. Kodama, and W. L. Qian, Phys. Rev. Lett. **101**, 112301 (2008).
[45] J. Takahashi *et al*., Phys. Rev. Lett. **103**, 242301 (2009).
[46] M. Luzum and J.-Y. Ollitrault, Phys. Rev. Lett. **106**, 102301 (2011).
[47] A. M. Poskanzer and S. A. Voloshin, Phys. Rev. C **58**, 1671 (1998).
[48] R. P. G. Andrade, F. Grassi, Y. Hama, and W.-L. Qian, arXiv:1008.4612 [nucl-th].
[49] J. Adams *et al*. (STAR Collaboration), Phys. Rev. Lett. **92**, 062301 (2004).
[50] A. Adare *et al*. (PHENIX Collaboration), Phys. Rev. Lett. **105**, 062301 (2010).
[51] C. Gombeaud and J.-Y. Ollitrault, Phys. Rev. C **81**, 014901 (2010).